Molecular Vision 2007; 13:1496-507 <http://www.molvis.org/molvis/v13/a166/>
Received 30 April 2007 | Accepted 13 August 2007 | Published 28 August 2007

Disruption of actin cytoskeleton causes internalization of $Ca_v1.3$ (alpha 1D) L-type calcium channels in salamander retinal neurons

Massimiliano Cristofanilli, Fengxia Mizuno, Abram Akopian

Department of Ophthalmology NYU School of Medicine, New York, NY

Purpose: To study the influence of actin cytoskeleton reorganization on the subcellular distribution of $Ca_v1.3$ L-type Ca^{2+} channels in salamander retinal third-order neurons.

Methods: Immunocytochemistry with confocal microscopy was used to demonstrate internalization of the $Ca_v1.3$ isoform of L-type voltage-gated Ca^{2+} channels in third-order retinal neurons. A specificity of antibody was confirmed with Western blotting and in control experiments preabsorbing antibody wit its respective peptide. Whole-cell patch clamp technique was applied to record L-type currents from ganglion cells in slice preparations in the presence of N- and P/Q type Ca^{2+} channel blockers.

Results: A high level of $Ca_v1.3$ labeling was present in cone photoreceptor terminals in the outer plexiform layer (OPL), as aggregates of puncta. Punctate $Ca_v1.3$ labeling was evident throughout the IPL and around the cell bodies in the outer nuclear (ONL), inner nuclear (INL) and on somas and axons of ganglion cells labeled with rhodamine-conjugated dextran. Doubly labeled sections for synaptophysin and $Ca_v1.3$ revealed colocalization in the OPL and IPL. Depolymerization of the actin cytoskeleton caused a dynamin-dependent internalization of $Ca_v1.3$ but not $Ca_v1.2$ subtype of voltage-gated Ca^{2+} channels in dissociated neurons. In ganglion cells, the inhibition of L-type Ca^{2+} currents by F-actin disrupters was mediated by Ca^{2+} channel internalization. Treatment with cytochalasin D protected retinal neurons against kainate-induced excitotoxicity.

Conclusions: Actin cytoskeleton dynamics plays an important role in the regulation of subcellular distribution and function of $Ca_v1.3$ L-type Ca^{2+} channels in salamander retinal neurons. Ca^{2+}-dependent actin depolymerization may serve as a negative feedback mechanism to reduce excessive Ca^{2+} influx and thereby protect neurons against glutamate-induced excitotoxicity.

Calcium influx through voltage-activated L-type channels triggers multiple intracellular signaling pathways that regulate diverse cellular processes in the vertebrate retina [1]. The main component of high voltage-activated L-type Ca^{2+} channel (Ca_v) is the pore-forming α_1 subunit, which is responsible for the principal biophysical and pharmacological properties of the channel. According to present nomenclature, the Ca_V1 subfamily ($Ca_V1.1$-$Ca_V1.4$) includes channels containing α_1S, α_1C, α_1D, and α_1F, all of which mediate L-type Ca^{2+} currents [2]. Each subtype mediates different functions and characterized by distinct pharmacological and electrophysiological properties and subcellular distributions [3].

Biochemical and immunocytochemical studies have demonstrated expression of $Ca_v1.2$ and $Ca_v1.3$ isoforms of L-type Ca^{2+} channels (hereafter $Ca_v1.3$) in retinal preparations of different species including salamander [4-9]. The $Ca_v1.4$ subtype is preferentially, but not exclusively [10] localized to the photoreceptor and bipolar cell terminals of mammalian retina [11], and mutations in gene encoding this channel subtype cause incomplete X-linked congenital stationary night blindness [12]. Investigation of the subcellular distribution and regulation of $Ca_v1.3$ in the retina is of special interest owing to its wide distribution in cell processes and somas, and its low threshold of activation and very slow inactivation [13], properties which makes these channels well suited for involvement in neurotransmitter release in ribbon synapses of photoreceptors and bipolar cells [14-16].

Trafficking of ion channels and postsynaptic ionotropic receptors has been the subject of extensive studies in recent years [17-19]. The agonist-induced internalization of N-type Ca^{2+} channels has been recently demonstrated in rat dorsal root ganglion neurons [20], and in chick sensory neurons [21]. Increasingly, it is recognized that ion channels in the surface membrane exist within highly coordinated assemblies that include proteins associated with the actin cytoskeleton. The disruption of channel-cytoskeleton interaction resulted in a G protein-mediated internalization of voltage-gated N-type Ca^{2+} channels in embryonic chick sensory neurons [22]. Hence, the actin cytoskeleton plays an important role in synaptic modulation and plasticity both by anchoring these proteins, and limiting their lateral movement in the membrane and by controlling endocytosis and the delivery of receptor and ion channel proteins into and out of the plasma membrane. Agents that interfere with the structure of the actin cytoskeleton have marked effects on ion channel and neurotransmitter receptor activities in the vertebrate retina [23,24]. Consequently, the

Correspondence to: Abram Akopian, NYU School of Medicine, Department of Ophthalmology, 550 First Ave, PHL 843 NYU School of Medicine, New York, NY 10016; Phone: 212-263-7603; FAX: 212-263-7602; email: aa3@nyu.edu

Dr. Cristofanilli is now at the Keck Center for Collaborative Neuroscience the State University of New Jersey at Rutgers.

remodeling of the actin cytoskeleton during different neuronal activities may be a determinant of synaptic strength by regulating the mobilization and the targeting of ion channels to their specific sites of function and modulation.

In the present study we investigated the effect of actin cytoskeleton reorganization on the subcellular localization of $Ca_v1.3$ channels in salamander retinal neurons. We found that actin depolymerization causes dynamin-dependent internalization of $Ca_v1.3$ channels in retinal neurons.

METHODS

Retinal preparation: The handling and the maintenance of animals met the National Institutes of Health guidelines and were approved by the Institutional Care and Use Committee at NYU School of Medicine. Salamanders (*Ambystoma tigrinum*) were anesthetized by immersion in a solution of tricaine methanosulfonate (100 mg/ml) until the animal no longer reacted to tactile stimulation; animals then were decapitated and double pithed. The eyes were cut in half, and the retina was dissected out for preparation of dissociated cells. Eyecups were used for preparation of cryostat sections.

Electrophysiology: The general procedures for preparing retinal slices used in patch clamp recording have been described elsewhere [23]. Whole-cell voltage clamp recordings were obtained using Patchmaster software and EPC-10 amplifier (HEKA Electronik, Germany) and analyzed with Igor Pro5 software. Whole-cell capacitance and series resistances were compensated automatically. Membrane currents were filtered at 1.0 kHz and sampled at 2.5 kHz. Summary data are presented as mean±SE. Statistical comparisons were done with Student's t-test and differences were considered significant at the $p<0.05$ level. The bath solution contained: NaCl 100 mM, KCl 3 mM, $CaCl_2$ 2 mM, $MgCl_2$ 2 mM, HEPES 10 mM, adjusted to pH 7.6 with NaOH. A standard voltage paradigm was used to elicit voltage-dependent L-type Ca^{2+} currents in the presence of tetrodotoxin (TTX; 1 μM), and tetraethylammonium chloride (TEA; 20 mM, replacing equimolar NaCl) in bath solution to block voltage-gated Na^+ and K^+ currents, respectively. To record L-type Ca^{2+} current, ω-conotoxin GVIA (800 nM) and ω-agatoxin IVA (1 μM) was included in the external solution to block N- and P/Q type Ca^{2+} currents, respectively. Calcium currents were recorded with 10 mM Ca^{2+} or Ba^{2+} in the external solution as a charge carrier. Calcium currents were recorded with low-resistance electrode (5-6 MΩ), filled with pipette solution consisting of (mM): 100 CsCl; 10 KCL; 0.5 $CaCl_2$, 2 $MgCl_2$, 0.5 EGTA, 2 ATP; 0.1 GTP and 10 HEPES, buffered to pH 7-4 with KOH. Cytochalasin B (cytB), and latrunculin B (latB), (Sigma-Aldrich, St. Louis, MO) was added to the patch pipette solution at final concentrations of 20 μM and 5 μM, respectively.

Immunostaining of retinal sections: After each treatment, eyecups were fixed with phosphate-buffered 4% paraformaldehyde (PFA) pH 7.3, dehydrated with 30% sucrose solution overnight at 4 °C, embedded in Tissue-Tek solution and sectioned at about 15 μm frozen sections on a cryostat. For immunostaining of $Ca_v1.3$ channel, sections were permeabilized with 0.1% Triton-X-100 for 5 min in PBS, preincubated in blocking solution (4% donkey serum 0.1% Triton-X-100 in PBS) for 1 h at room temperature (RT) then incubated over night at 4 °C with polyclonal rabbit anti-$Ca_v1.3$ antibody recognizing intracellular epitope (amino acids 859-875) of rat brain voltage-gated calcium channel (Chemicon, Temecula, CA), diluted 1:200 in blocking solution. Retinal sections were rinsed three times in PBS and incubated in secondary antibodies diluted in PBS: anti-mouse Cy3, 1:500 (Jackson Immunoresearch, West Grove, PA); anti-rabbit Alexa Fluor 488, 1:1,000 (Molecular Probes, Eugene, OR), then sections were rinsed three times in PBS and coverslipped with Prolong Gold Antifade Mounting Medium (Invitrogen, Carlsbad, CA). To visualize actin filaments, sections were washed, repermeabilized, pre-incubated for 30 min with 3% BSA (0.1% Triton-X in PBS), and incubated for 2 h at RT with Alexa Fluor 488-phalloidin (Invitrogen, Carlsbad, CA) diluted in the BSA-Triton-X solution with final phalloidin concentration of 0.2-0.3 μM. After extensive rinsing, the tissues were mounted with Vectashild (Vector Burlingame, CA) and observed with a confocal laser-scanning microscope Nikon Eclipse C-1 (Nikon, Japan). Single plane images were acquired using 60x or 100x oil-immersion objective lens and EZ-C1 (Nikon) software. Images from controls and treated samples were obtained with the same scanning parameters, and were processed using deconvolution software AutoDeblur (Autoquant Image Inc.), and Adobe Photoshop (version 7.0). To control for day-to-day variations in staining intensity, treated specimens were always compared with control prepared the same day under identical conditions of fixation, permeabilization, staining, and microscopy.

Immunostaining of dissociated cells: Isolated retinas were incubated for 1 h at RT with papain solution (14 U/ml, Worthington Biochemicals, Lakewood, NJ) in 14 ml 0.5 mM Ca/25 mM $NaHCO_3$ Ringer solution containing 6 mg cysteine, 1 mM Na-pyruvate, 16 mM D-glucose, and 1.1 mM EDTA, oxygenated with 5% CO_2/95% O_2 for 30 min at RT. After rinses retinas were dissociated in DMEM (Invitrogen) using a wide-bore 5 ml pipette, plated on poly-L-lysine coated coverslips, and left to settle for 30-45 min before treatments. Cells were then treated for 30 min with either latA (5 μM) or cytD (10 μM), membrane-permeable analogs of latB and cytB, respectively (both from Biomol International, Plymouth, PA) and fixed with 4% PFA. To block endocytosis, cells were preincubated for 1 h with 50 μM DIP. The protocol for staining F-actin and $Ca_v1.3$ was similar to the one described above for retinal slices. Polyclonal rabbit anti-$Ca_v1.2$ antibody (Alomon Labs, Israel) was diluted 1:500 in blocking solution. To block endocytosis, cells were preincubated for 1 h with myristoylated dynamin-inhibitory peptide (Tocris, Ellisville, MO) prior to fixing and labeling with $Ca_v1.3$ antibody. Coverslips were mounted with Prolong Gold Antifade Mounting Medium (Invitrogen, Carlsbad, CA) and observed with a confocal laser-scanning microscope as describe above. Changes in $Ca_v1.3$ distribution were assessed by measuring the optical densities separately for the whole area and the cytosolic region using Metamorph software (Universal Imaging Co. Downington, PA). The membrane fluorescence (F_m) was de-

fined as the difference between total and cytosolic intensity (F_c), and the internalized channels were quantified by measuring the ratio of F_c/F_m. To quantify the changes in the actin network, scans of pixel intensity were performed by linescan using Metavue software (Universal Imaging Co.) and the intensity profile was obtained along a line drawn through the cell perikarya. All pooled data are presented as mean±SE. Levels of significance were assessed using Student's paired t test with $p<0.05$ considering as significant.

Western blotting analysis: Dissociated retinal cells were placed in an Eppendorf tube and treated with 20 μM cytD for 30 min. Cells were centrifuged at 1000 RPM for 5 min at 4 °C and the resulting pellets washed 3 times with ice-cold Ringer solution, then resuspended in 100 μl of hypotonic buffer A (20 mM Tris, pH 8.0, 1 mM EDTA), 1% proteases inhibitor cocktail (Sigma, St Louis, MO), 1 mM dithiothreitol. Protein for Western blots was extracted and measured using a BCA protein determination kit (Sigma). Equal amounts of proteins were run on a SDS-PAGE gel, verified by Ponceau and/or Coomassie stains, transferred to a nitrocellulose membrane, blocked with 5% nonfat dried milk in Tris Buffered Saline with 0.1% Tween 20 (TBS/T), and probed with $Ca_v1.3$ anti-

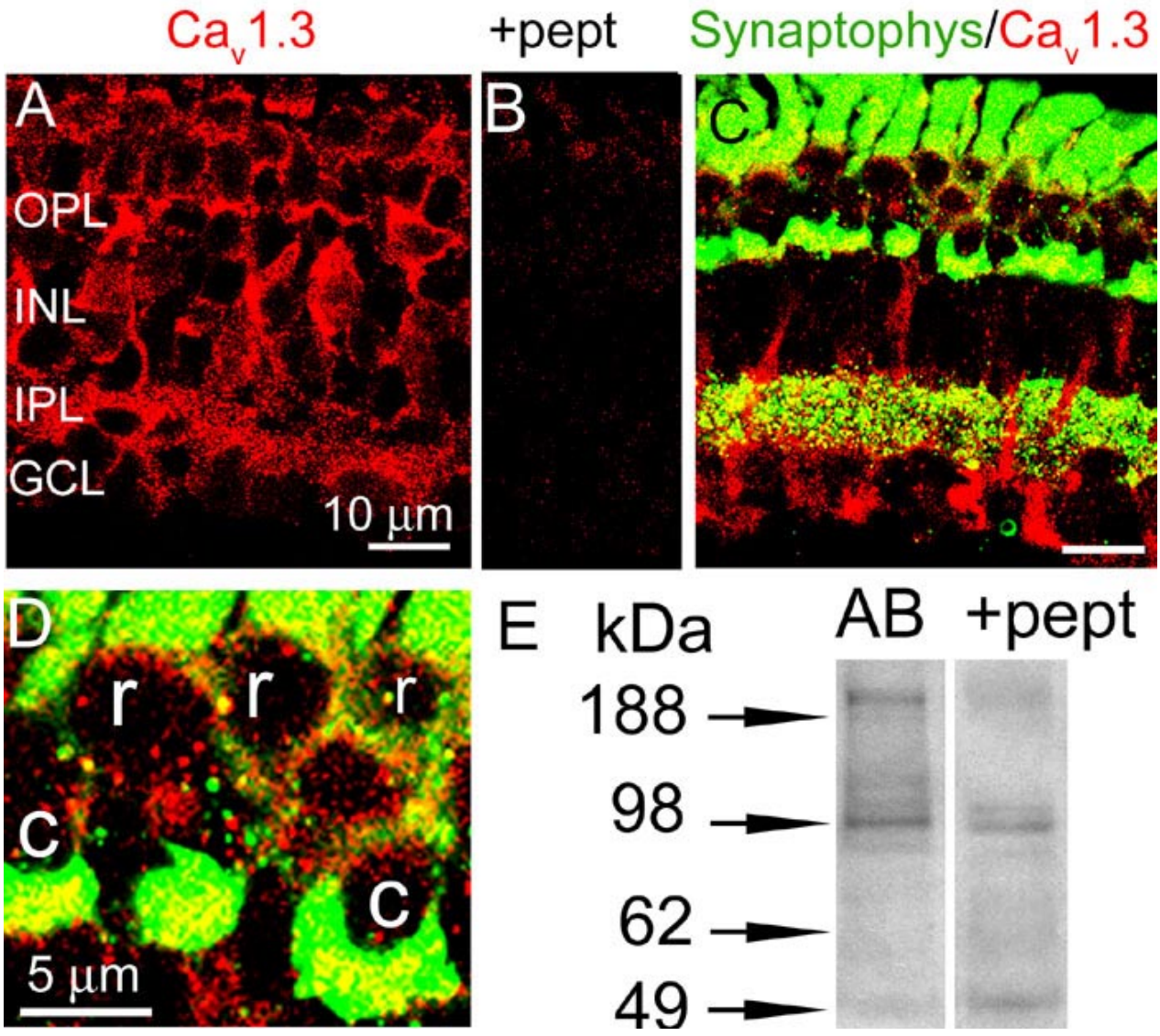

Figure 1. Localization of $Ca_v1.3$ L-type Ca channels in salamander retina. **A**: In salamander retinal slices $Ca_v1.3$ labeling was present in the outer plaxiform layer (OPL), inner plexiform layer (IPL) and on somas of cone photoreceptors and cells in the inner nuclear layer (INL), and ganglion cell layer (GCL). **B**: Preabsorbtion of antibody with respective peptide revealed only feint staining in photoreceptor inner segments. **C**: Double labeling with anti-synaptophysin (green) and anti-$Ca_v1.3$ (red) antibodies revealed aggregates of $Ca_v1.3$ puncta colocalized with synaptophysin in the OPL. Numerous puncta in the IPL also showed colocalization. **D**: Magnified image of OPL area shown in **C**, indicates localization of $Ca_v1.3$ channels in cone (c) photoreceptor terminals. **E**: In western blot analysis $Ca_v1.3$ antibody provided major bond around 200 kDa and a minor one around 140 kDa (n=4, 3 different retinal preparations). Preabsorption of anti- $Ca_v1.3$ with control peptide (+ pept) abolished the 200 kDa band.

body (Chemicon) diluted 1:200 in 1% BSA in TBS/T. After washing, the membranes were incubated with horseradish peroxidase-conjugated secondary antibodies (Pierce) and detected using the Western Lighting Chemiluminescence kit (PerkinElmer Life Science).

Live/dead assay: After the enzymatic treatment with papain, isolated retinas were washed, placed in 1 ml centrifuge tube containing 0.5 ml Ringer solution and cells were dissociated by gentle trituration. Following centrifugation (at 500xg for 3 min) the supernatant solution was removed and cell pellet was incubated for 30 min with either Ringer solution or Ringer solution containing 20 μM cytD in room temperature. Samples then were washed (3x5 min), exposed for 30 min to 100 μM kainite, and then washed again for 2 h. After another centrifugation the cell pellet in the tube was loosen by sharply tapping the tube; 200 ml of dye containing 2 μM calcein-AM and 4 μM ethidium homodimer (Live/Dead assay, Molecular Probes, Eugene, OR) was added and incubated in complete darkness for 30 min. Cells were pelleted by centrifugation and supernatant solution was removed to avoid carry-over of dye. Following resuspension in fresh buffer solution, 10 ml of cell suspension was plated in the Bright-Line chamber (Hausser Scientific). Fluorescent images were obtained by laser scanning confocal microscope and cells were counted directly. The percentage of viable cells (normalized to control) was calculated as: the (number of live cells/number of total cells) x 100. All data are expressed as mean±SE. Significance of differences between groups was assessed by Student paired t test.

Labeling of retinal ganglion cells: Tetramethylrhodamine-dextran (Mw 3000, Molecular Probes) was used to label axonal fibers and ganglion cell somas through the cut of optic nerve. A few crystal of tracer were placed on a freshly cut optic nerve and the eyecup with attached tracer was stored at 4 °C overnight. The retina with labeled ganglion cells was then enzymatically treated for further cell dissociation.

RESULTS

Distribution of $Ca_v1.3$ channels in salamander retina: In vertical cryostat sections of salamander retina, the labeling for $Ca_v1.3$ was present in both OPL and IPL, as well as in nuclear layers (Figure 1A). Punctate $Ca_v1.3$ labeling was evident throughout the IPL and around the cell bodies in the ONL, the INL and the GCL. In the OPL labeling was present as aggregates of puncta, as well as numerous puncta. In addition, a large population of radially oriented elements extending from the OPL to the GCL expressed intense $Ca_v1.3$ immunoreactivity. Double immunolabelling for $Ca_v1.3$ and GFAP (glial cell marker) revealed colocalization of these epitopes in the soma and processes of retinal Muller cells (not shown). Control sections reacted with Cav1.3 antibody preabsorbed with

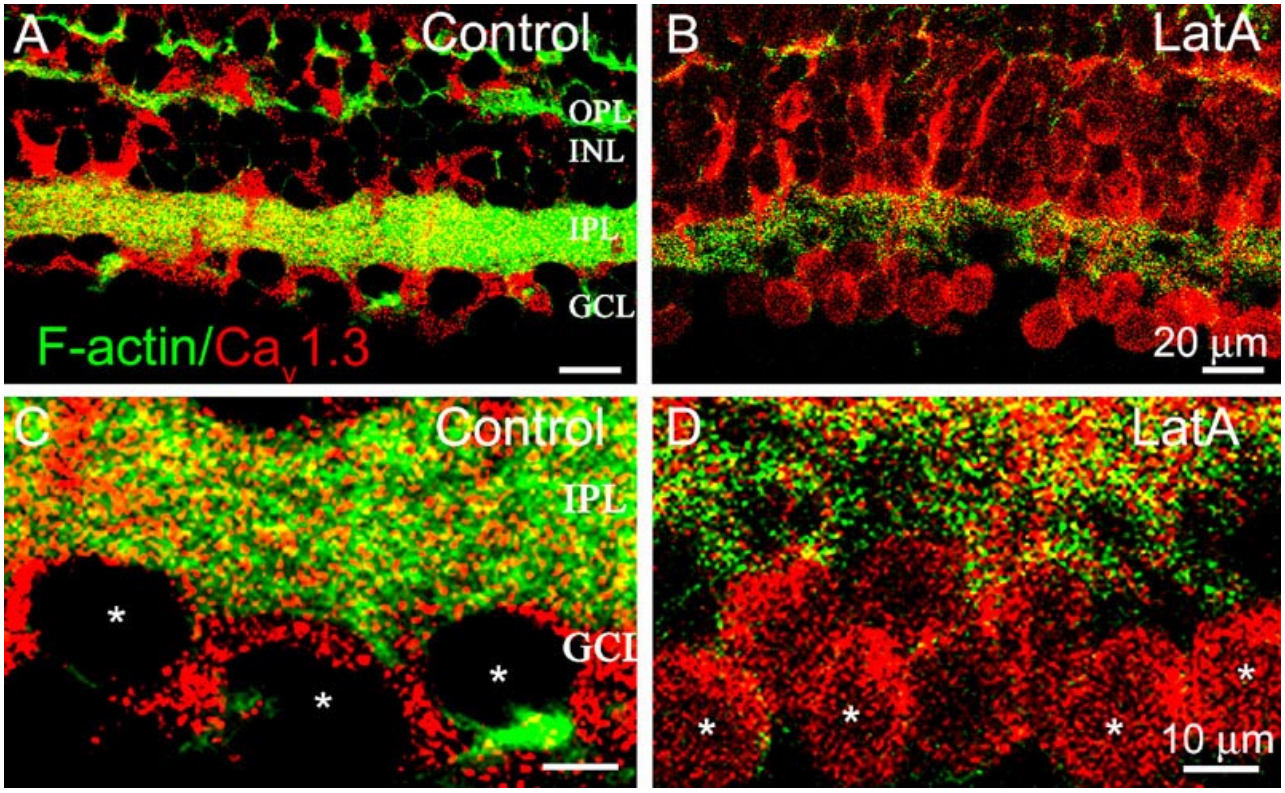

Figure 2. Effect of latrunculin A on distribution of $Ca_v1.3$ channels in retinal slices. **A**: Distribution of $Ca_v1.3$ channels in control slices. Vertical sections are double labeled with anti-$Ca_v1.3$ antibody (red) and Alexa-Fluor488-phalloidin (green) to visualize F-actin. **B**: Pretreatment of slices for 30 min with 5 μM latA reduced intensity of phalloidin staining, indicative of F-actin disruption, and increased $Ca_v1.3$ labeling in the cell cytoplasm. **C**, **D**: Magnified images of ganglion cell layer (GCL) in control, and latA-treated retinal slices show increased $Ca_v1.3$ labeling in cell cytoplasm (asterisks), following F-actin disruption.

immunogen peptide (Figure 1B), or labeling of slices with secondary antibody alone (not shown), displayed complete loss of specific immunolabeling. In whole-mount retinal preparations $Ca_v1.3$ labeling was localized to somas and axons of ganglion cells, which were visualized by retrograde labeling with rhodamine-conjugated dextran from the optic nerve section (not shown).

Immunofluorescent confocal images of vertical sections doubly labeled for synaptophysin and $Ca_v1.3$ revealed presence of $Ca_v1.3$ channels in photoreceptor terminals in the OPL (Figure 1C). Apparent labeling for synaptophysin in photoreceptor inner and outer segments was due to nonspecific autofluorescence, characteristic for salamander retina. The high power image of OPL shows that $Ca_v1.3$ channels are primarily localized to cone photoreceptor terminals (Figure 1D). The presence of numerous puncta adjacent to, but not associated with, synaptophysin labeling, suggests an additional postsynaptic localization for $Ca_v1.3$ channels. Although numerous puncta in the IPL show double labeling for $Ca_v1.3$ and synaptophysin, most labeling was not colocalized, indicative of both presynaptic and postsynaptic localization of $Ca_v1.3$ channels in the IPL. The expression of $Ca_v1.3$ channel protein in salamander retina was confirmed by western blotting (Figure 1E), showing that the anti-$Ca_v1.3$ antibody recognized a protein with a molecular mass around 200 kDa, corresponding to $Ca_v1.3$ channel protein observed in molecular studies

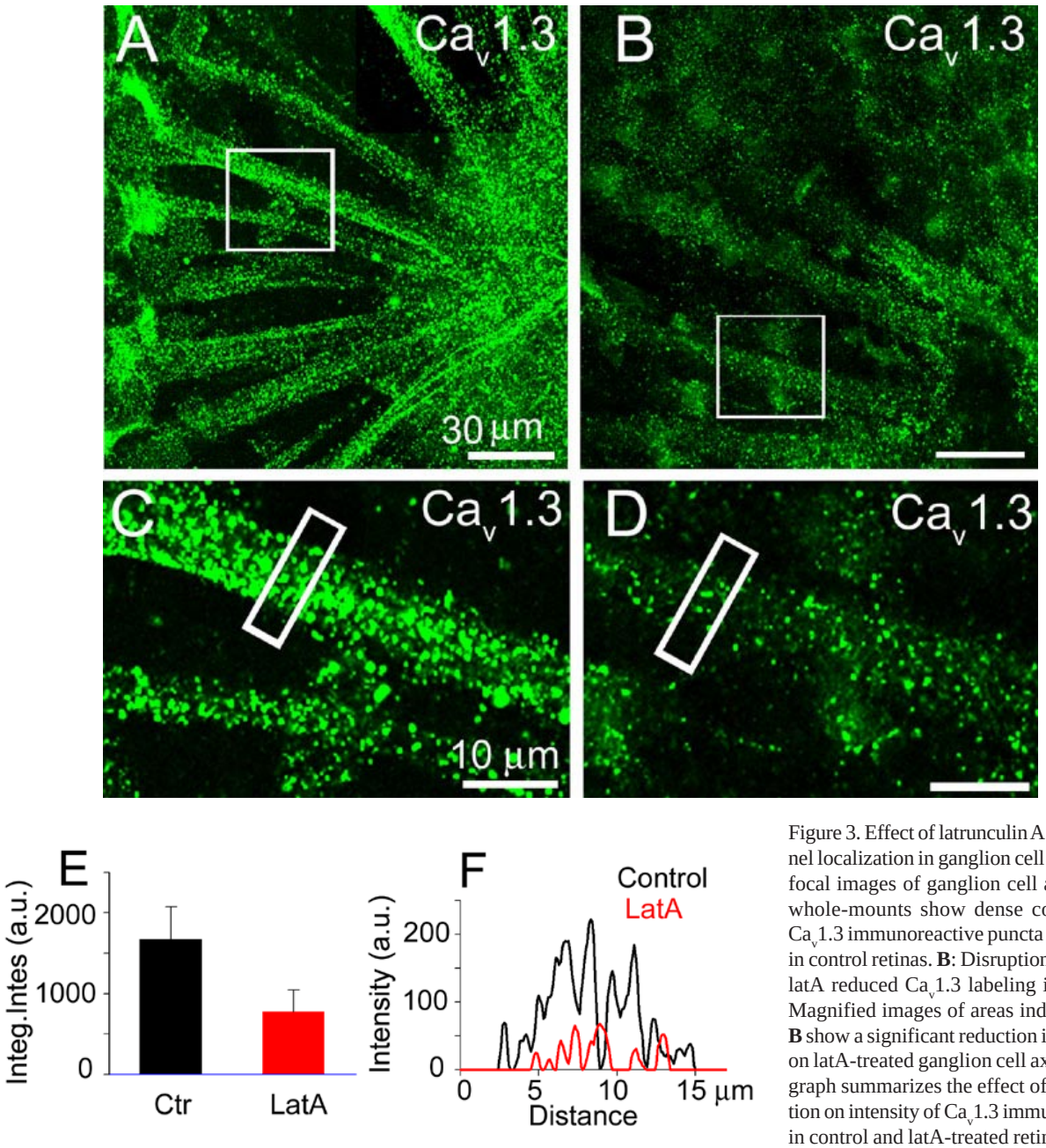

Figure 3. Effect of latrunculin A on $Ca_v1.3$ channel localization in ganglion cell axons. **A**: Confocal images of ganglion cell axons in retinal whole-mounts show dense concentration of $Ca_v1.3$ immunoreactive puncta along the axons in control retinas. **B**: Disruption of F-actin with latA reduced $Ca_v1.3$ labeling in axons. **C**, **D**: Magnified images of areas indicated in **A** and **B** show a significant reduction in $Ca_v1.3$ puncta on latA-treated ganglion cell axons. **E**: The bar graph summarizes the effect of F-actin disruption on intensity of $Ca_v1.3$ immunofluorescence in control and latA-treated retinas. **F**: Intensity profiles of $Ca_v1.3$ immunofluorescence from indicated areas in **C** and **D**.

[25]. Preabsorption of anti- $Ca_v1.3$ with control peptide abolished the 200 kDa band (+ pept). The broad distribution of $Ca_v1.3$ channels in both synaptic layers and somas of different cell types, including ganglion cells and their axons, suggest multifunctional roles for these channels in the retina.

Effect of latrunculin A and cytochalasin D on $Ca_v1.3$ channel distribution in retinal slices: To study the influence of cytoskeletal reorganization on the distribution of $Ca_v1.3$ channels, we treated retinal slices either with latA or cytD, then fixed and double stained with anti- $Ca_v1.3$ antibody and Alexa-Fluor488-phallodin, to monitor changes in the actin cytoskeleton organization. In control slices, $Ca_v1.3$ labeling outlined the cell bodies in the INL, the ONL, and the GCL (Figure 2A). The disruption of F-actin by latA, which was evident by the faint intensity of phalloidin staining, resulted in an increase in $Ca_v1.3$ labeling in the cytoplasm of these cells (Figure 2B). The magnified confocal immunofluorescence images of GCL clearly show the increased cytoplasmic $Ca_v1.3$ labeling in F-actin disrupted ganglion cells (Figure 2D, asterisks) compared to control cells (Figure 2C). A qualitatively similar effect was observed when F-actin was disrupted with cytD (not shown).

Disruption of F-actin also dramatically changed the distribution of $Ca_v1.3$ channels in ganglion cell axons. In the representative experiment illustrated in Figure 3 retinal whole-mounts were labeled with anti- $Ca_v1.3$ antibody under control conditions (Figure 3A) and after a 30 min preincubation with 5 μM latA (Figure 3B). Magnified immunofluorescence confocal images (areas in Figure 3A,B) clearly show the dense localization of $Ca_v1.3$ labeling along axons in control retina (Figure 3C), which was significantly reduced following F-actin disruption (Figure 3D). To quantify these changes, we measured the integrated intensities of $Ca_v1.3$ fluorescence in bundles of axons in control and treated retinas (Figure 3E). Depolymerization of F-actin reduced fluorescence intensity of axonal $Ca_v1.3$ immunolabeled puncta by about 50%. The intensity profiles obtained from indicated areas in Figure 3C,D are illustrated in Figure 3F.

Depolymerization of F-actin caused internalization of $Ca_v1.3$ channels in third-order retinal neurons: Because of difficulties in studying detailed changes in subcellular distribution of $Ca_v1.3$ in a retinal slice preparation, further studies were carried out on acutely dissociated retinal neurons. Owing to their characteristic morphology we could distinguish dissociated photoreceptors, horizontal cells and Muller cells from third order neurons (ganglion/amacrine cells), which were included in all quantitative analyses. Confocal fluorescence images through the center of the neuronal perikarya show that under control conditions $Ca_v1.3$ labeling appeared as puncta outlining cell somas, indicative of a surface localization (Figure 4A, left panel). $Ca_v1.3$ labeling was concentrated in the somatodendritic region. Double staining with Alexa-Fluor 488 phalloidin revealed colocalization of F-actin and $Ca_v1.3$ on the surface membrane and proximal processes (Figure 4A, middle and right panels). Exposure of dissociated cells for 30

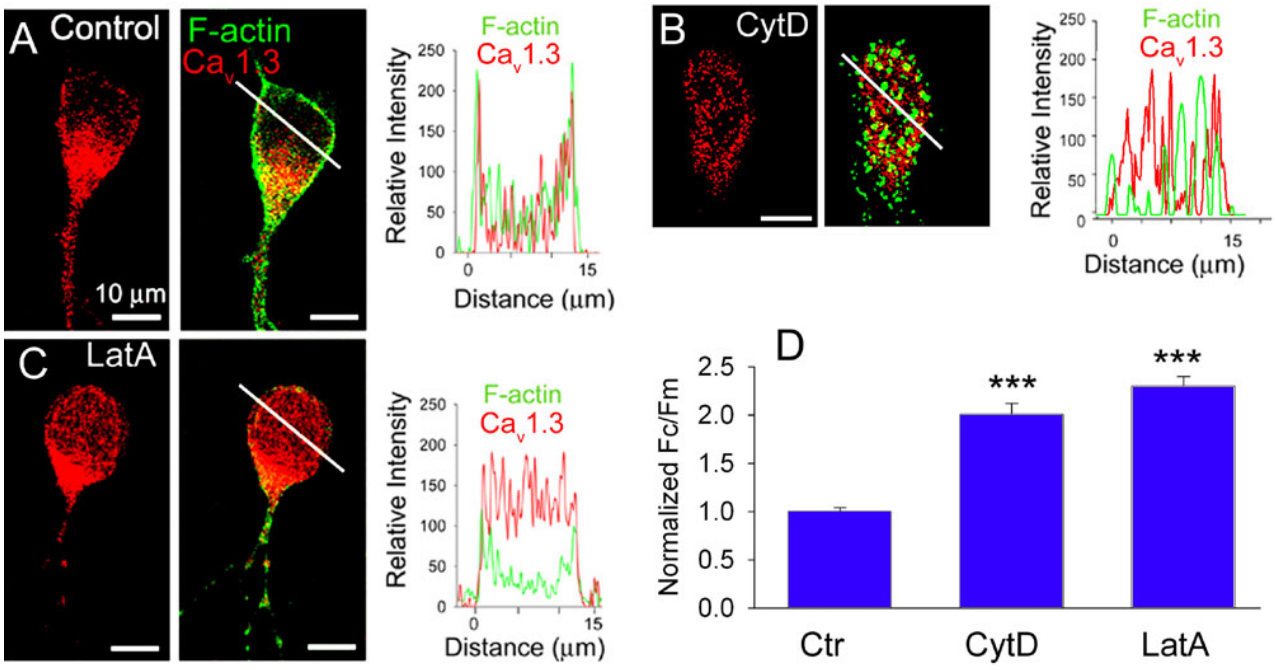

Figure 4. Depolymerization of F-actin causes $Ca_v1.3$ channel internalization in third-order retinal neurons. **A**: Subcellular localization of $Ca_v1.3$ channels (red) in third-order retinal neurons double stained with Alexa-Fluor488-phalloidin (green, middle panel). Intensity profiles show localization of $Ca_v1.3$ primarily on the surface membrane (right panel). **B**, **C**: Depolymerization of F-actin by either 10 μM cytD, or 5 μM latA reduced $Ca_v1.3$ labeling on the surface and increased it in the cytoplasm, as was evident from intensity profiles (right panels) obtained along the white lines. **D**: The bar graph summarizes effects of F-actin disrupters on internalization of $Ca_v1.3$ channel. F_c and F_m represent the cytoplasmic and the membrane immunofluorescence, respectively. Each column represents the mean±SE (n=30-50, 3-5 independent experiments, triple asterisks $p<0.0001$).

min to latA (5 μM) or cytD (10 μM) resulted in actin depolymerization, as is evident from a significant reduction in fluorescence intensity of Alexa-Fluor 488-phalloidin (Figure 4B,C, middle panels). The disruption of F-actin reduced $Ca_v1.3$ labeling on the surface and increased it in the cytoplasm (Figure 4B,C, left panels). Intensity profiles for F-actin and $Ca_v1.3$ along the indicated white lines highlight that the peak of fluorescence intensity occurs at the plasma membrane for both F-actin and $Ca_v1.3$ in control untreated cells, with a lower intensity seen in the cytoplasm (Figure 4A, right panel). Following F-actin disruption the fluorescence intensities of phalloidin and $Ca_v1.3$ were reduced on the surface (Figure 4B,C, two peaks in the right panels), associated with an increase in $Ca_v1.3$ labeling in the cytoplasm (area between peaks).

To quantify changes in subcellular distribution of $Ca_v1.3$ channels, the integrated fluorescence intensity was measured in the cytoplasmic area (F_c), and the surface membrane (F_m) and the F_c/F_m ratio was used to assess the degree of internalization [22]. The disruption of F-actin either by latA or cytD increased the mean F_c/F_m ratio for $Ca_v1.3$ to1.4±0.1 and 1.2±0.1, respectively, from 0.6±0.04 in control cells (n=20 each, $p<0.003$, 3 independent experiments). The bar graph in Figure 4D shows normalized F_c/F_m under different experimental conditions, indicating that actin depolymerization caused internalization of $Ca_v1.3$ L-type Ca channels in third-order neurons of salamander retina. Interestingly, the disruption of F-actin by cytD failed to induce any significant internalization of $Ca_v1.2$ isoform of L-type channels in retinal neurons (not shown). The F_c/F_m ratio for $Ca_v1.2$ was changed from 0.7±0.05 in control, to 0.8±0.05 in cells treated with cytD (n=30). There was no apparent immunoreactivity evident when each of the two primary antibodies was preadsorbed with its respective control peptide.

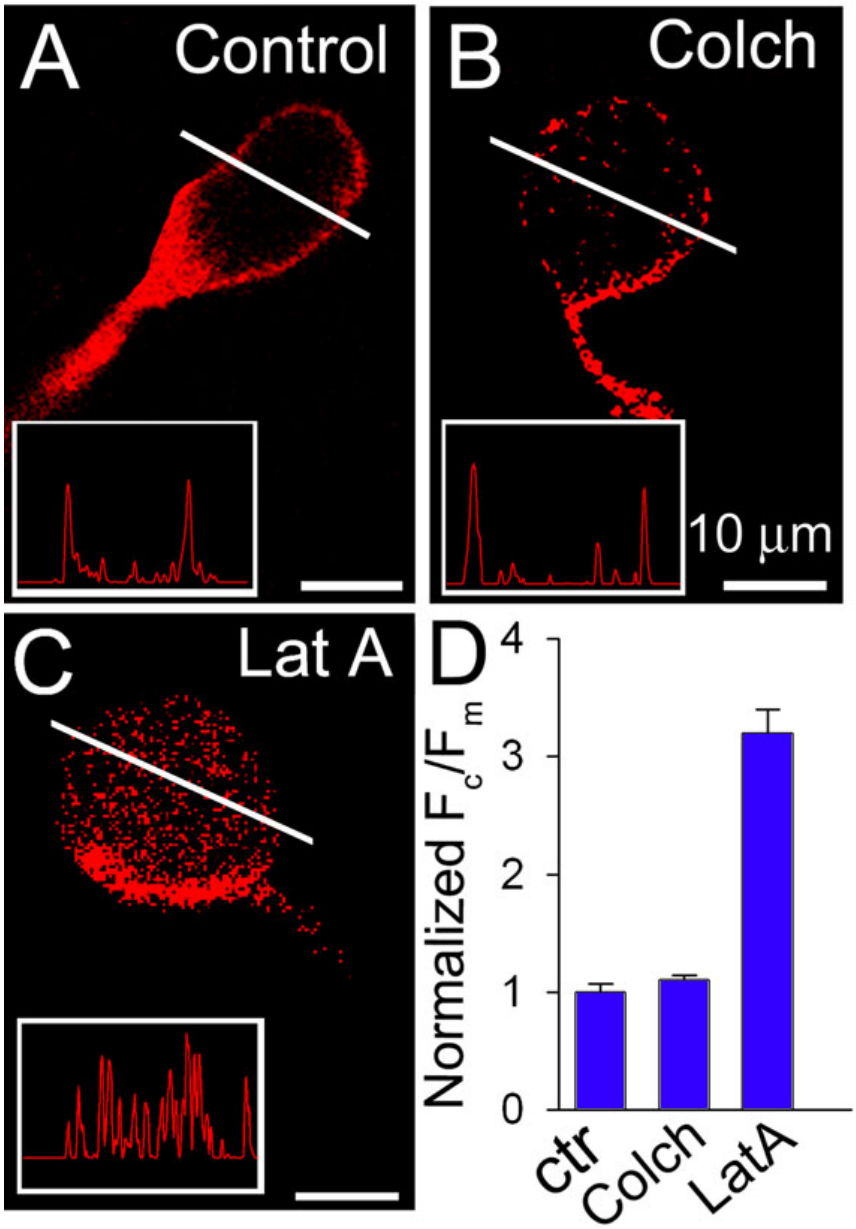

Figure 5. Disruption of microtubules has no effect on distribution of $Ca_v1.3$ channels. **A**: Subcellular localization of $Ca_v1.3$ channels in control cells, **B** in cells preincubated for 30 min with 50 μM colchicines, a microtubule disrupter, or **C** with 5 μM latA, to disrupt F-actin. Latrunculin A, but not colchicine increased cytoplasmic $Ca_v1.3$ labeling, as is evident from intensity profiles obtained along the white lines (insets). **D**: The bar graph summarizes effects of latA and colchicine on $Ca_v1.3$ channel internalization. Each column represents the mean±SE (n=20, 3 independent experiments $p<0.005$).

Next we tested whether the disruption of microtubules alters the subcellular distribution of $Ca_v1.3$ channels. Dissociated cells were incubated for 30 min either in normal Ringer solution, or a Ringer solution containing either latA (10 μM), or microtubule disrupting agent colchicine (20 μM). Thereafter the cells were fixed and stained with anti $Ca_v1.3$ antibody. Treatment of cells with colchicine had no significant effect on thesubcellular distribution of $Ca_v1.3$. The confocal images in Figure 3 show qualitatively similar surface localization of $Ca_v1.3$ labeling in control (Figure 5A) and colchicine-treated cells (Figure 5B). In contrast, parallel treatment of cells with latA caused characteristic internalization of $Ca_v1.3$ channels (Figure 5C). Intensity profiles of $Ca_v1.3$ fluorescence along the indicated white bars are illustrated for each cell (insets). Quantification (Figure 5D) revealed that the mean F_c/F_m ratio for cells incubated in normal Ringer solution, or treated with colchicine, or latA were 0.39±0.07, 0.43±0.04 ($p>0.5$), and 1.3±0.2 ($n=20$, $p<0.001$; 3 experiments), respectively.

Dynamin-dependence of $Ca_v1.3$ channel internalization: It is becoming increasingly evident that dynamin-dependent endocytosis of membrane receptor and channel proteins is an important means of controlling the cell surface expression, and hence the function, of these proteins [26]. To examine whether F-actin-regulated internalization of $Ca_v1.3$ channels depends on dynamin activity, we used a myristoylated dynamin-inhibitory peptide (DIP) that blocks endocytosis by interfering with the binding of amphiphysin with dynamin, an interaction that is considered important for endocytosis to occur [27,28]. In the representative experiment illustrated in Figure 6, dissociated cells were preincubated either in normal Ringer solution (Figure 6A,C), or in solution containing 50 μM DIP (Figure 6B,D) for 1 h prior to exposure for 30 min to

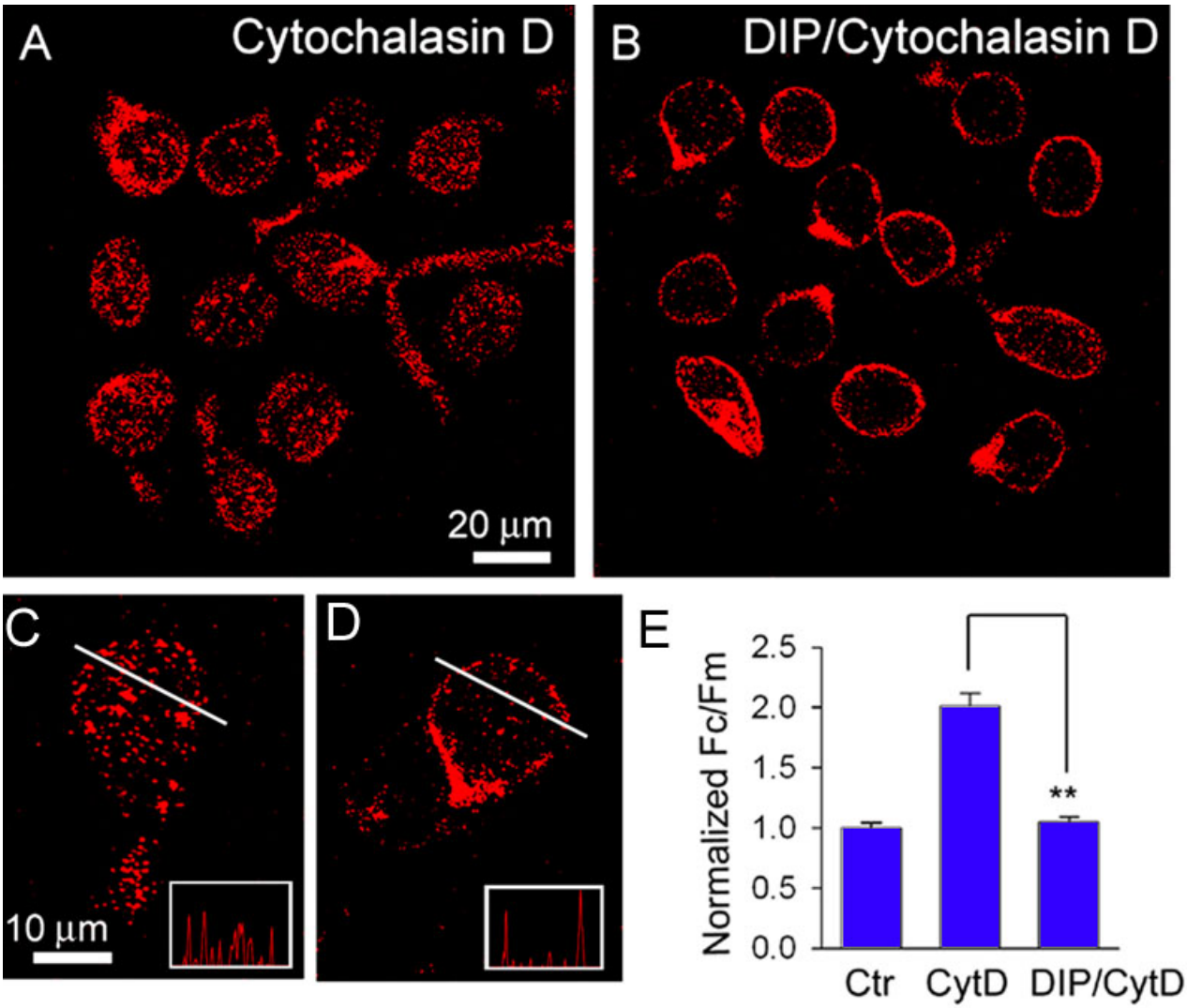

Figure 6. Internalization of $Ca_v1.3$ channel is dynamin-dependent. **A**: Effect of cytD on subcellular localization of $Ca_v1.3$ channels in control cells, and **B** in cells pre-treated for 60 min with 50 μM myristoylated dynamin inhibitory peptide (DIP). Inhibition of endocytosis by DIP attenuated the effect of cytD on $Ca_v1.3$ channel internalization. Intensity profiles for control (**C**) and DIP-treated (**D**) cells are illustrated in insets. **E**: The bar graph summarizes the effect of DIP on cytD-induced $Ca_v1.3$ channel internalization. Each column represents the mean±SE ($n=30$, 3 independent experiments, $p<0.01$).

20 μM cytD. Cells were then fixed and labeled with anti-$Ca_v1.3$ antibody. Block of endocytosis by DIP attenuated the effect of cytD on $Ca_v1.3$ internalization, reducing the mean F_c/F_m ratio from 2.03±0.12 in untreated cells, to 0.62±0.04 in cells treated with DIP (n=30, p<0.005). Intensity profiles along the indicated white lines (Figure 6A,B, insets), show reduced cytoplasmic $Ca_v1.3$ labeling in DIP-treated cells compared to control cells. The bar graph in Figure 6C shows normalized (to control) F_c/F_m ratios under two different experimental conditions, indicating that in salamander retinal neurons $Ca_v1.3$ L-type Ca^{2+} channels undergo a dynamin-dependent internalization triggered by F-actin disruption.

Correlation between Ca^{2+} channel internalization and inhibition of I_{Ca} by F-actin disrupters

We reported earlier an inhibition of L-type Ca^{2+} currents following F-actin depolymerization in salamander retinal gan-

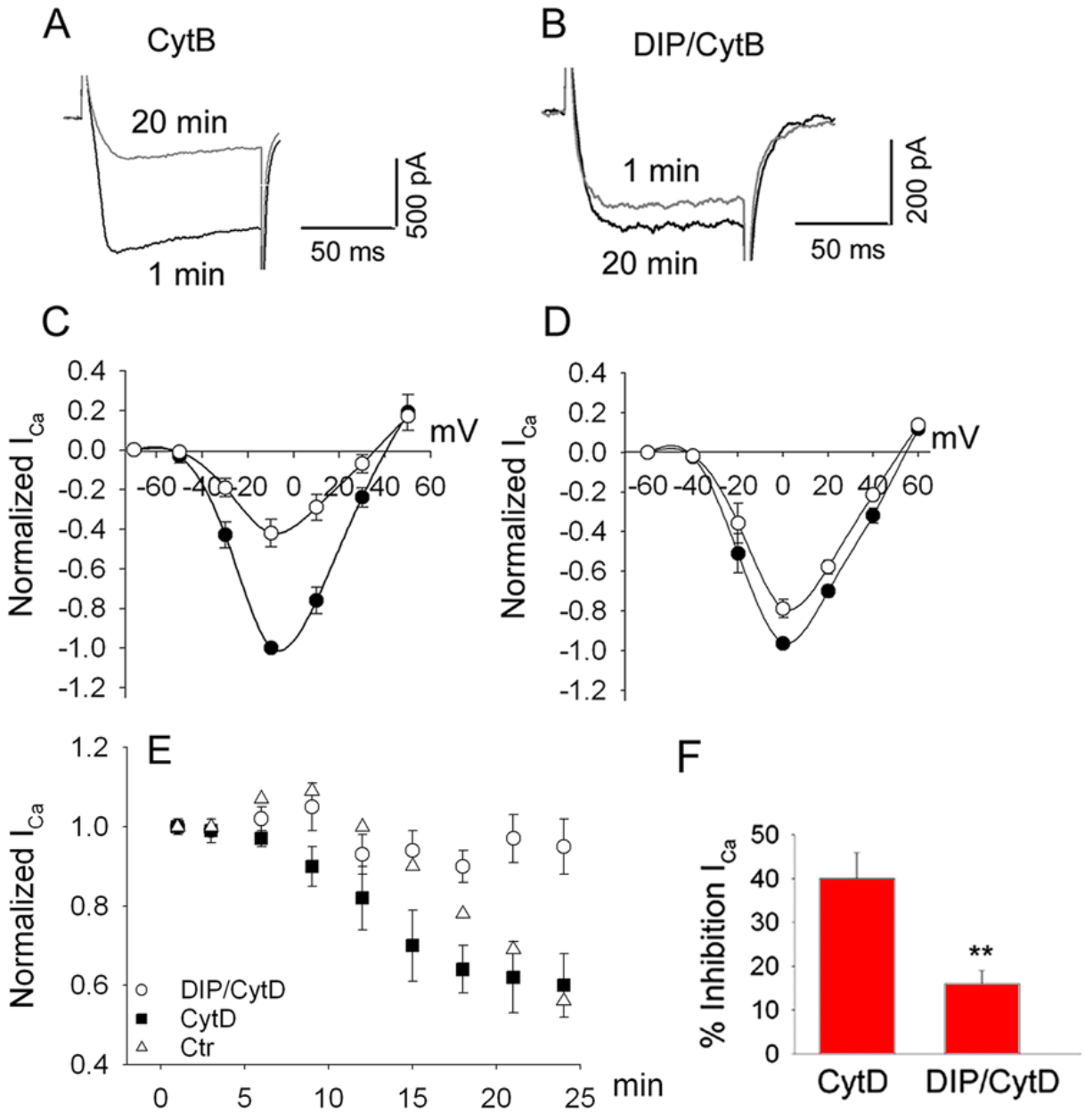

Figure 7. Correlation between $Ca_v1.3$ channel internalization and inhibition of L-type Ca current by cytochalasin B in retinal ganglion cells. **A**: L-type Ca currents (I_{Ca}) recorded from ganglion cells with the patch pipette containing 10 μM cytB in control slices, and **B** in slices preincubated for 60 min with 50 μM dynamin inhibitory peptide (DIP). Traces are peak I_{Ca} recorded in response to a depolarizing step from -70 to 0 mV at indicated times after the membrane rupture. **C**: Corresponding normalized I-V relationships obtained from ganglion cells within 1-2 min of membrane rupture (closed circles), and after 20-25 min (open squares) in control slices, and **D** in slices pretreated with DIP. **E**: Time course of peak I_{Ca} changes by cytB in control and DIP-treated ganglion cells. **F**: The bar graph summarizes data, indicating that block of endocytosis by DIP attenuated the inhibitory action of cytB on L-type I_{Ca}. Columns represent the mean±SE (n=6, p<0.005).

glion cells [20]. Our present results suggest that this inhibition might be caused by a reduction in the number of channels on surface membrane due to internalization. To test this hypothesis, we pretreated retinal slices for 30 min with dynamin-inhibitory peptide (DIP) and examined the effect of F-actin depolymerization on I_{Ca}. Whole-cell L-type currents were recorded by applying depolarizing pulses from -50 to +30 mV, in 10 or 20 mV increments, from a holding potential of -70 mV in the presence of W-conotoxin GVIA (800 nM), and ω-agatoxin IVA (1 μM) in the bath solution to block N- and P/Q type Ca currents, respectively. The patch pipette solution contained cytB (20 μM). Calcium currents recorded after 20-30 min in whole-cell mode were compared with those recorded within 1-2 min of membrane rupture. Representative traces in response to depolarizing step from -70 to 0 mV in control and DIP-treated cells are illustrated in Figure 7A. The disruption of F-actin significantly reduced peak I_{Ca} by 40±5% (n=10, $p<0.05$) in control slices. The block of endocytosis by DIP attenuated the inhibitory effect of F-actin disrupters to 12±3% (n=6, $p<0.05$). The corresponding I-V relationships in Figure 7B indicate that the reduction in peak amplitude in control and DIP-treated cells was not associated with changes in the voltage-dependence of the current. Normalized peak I_{Ca} recorded each 1 min during 20-25 min in whole-cell mode from ganglion cells in control (closed circles) and DIP-treated (open squares) slices are illustrated in Figure 7E. Notably, 3 out of 9 cells treated with DIP showed a about 30% increase in peak I_{Ca} in the presence of cytB (not included in the statistical analysis). The bar graph in Figure 7F summarizes these data indicating that block of endocytosis attenuated internalization of $Ca_v1.3$ channels by F-actin disrupters.

Possible implication in neuroprotection: Unrestrained Ca^{2+} influx through voltage-gated Ca channels can injure and kill neurons, a mechanism contributing to the ganglion cell death in glutamate-induced excitotoxicity [29]. Cytoskeleton-regulated internalization of Ca channels might increase cell viability by reducing the number of functional channels on plasma membrane, thereby reducing the amount of Ca entering into the cells. To test this proposition, dissociated retinal neurons were incubated for 1 h either in normal Ringer solution (Figure 8A), or in Ringer solution containing 10 μM cytD then both samples were exposed for 30 min to 100 μM kainate. Following a 2 h wash with normal Ringer solution, a live/dead assay was carried out. Quantification of the relative proportions of live and dead cells after kainate application (Figure 8B) revealed higher, 90±3% survival in cell populations treated with cytD compared to 75±2% in untreated cells.

DISCUSSION

In the present study we found, for the first time, that depolymerization of the actin cytoskeleton causes a dynamin-dependent internalization of $Ca_v1.3$ subtype of voltage-gated Ca channels in retinal neurons. We also showed that the inhibition of I_{Ca} by F-actin disrupters was mediated (at least partially) by Ca channel internalization.

$Ca_v1.3$ channels have been localized to the cone and bipolar cell terminals [4,9,30], as well as to cell bodies and processes of amacrine, ganglion and Müller cells [7,8] in retinal preparations of different species. Presence of $Ca_v1.3$ labeling in ganglion cell somas and axons marked by rhodamine-dextran (Figure 2B,C) is in agreement with earlier study on salamander retina [8]. Because of their unique biophysical characteristics (low threshold of activation and very slow inactivation) $Ca_v1.3$ channels have been implicated in neurotransmitter release in cone and bipolar cells terminals, where they translate the electrical responses of photoreceptors into graded, calcium-dependent release of the excitatory neurotransmitter, glutamate [9,14-16]. Calcium channels on the soma, on the other hand, could mediate Ca^{2+} influx, which is necessary for normal neuronal functions (e.g., triggering distinct Ca-dependent cellular processes), whereas the axonal Ca currents may regulate the firing rate of propagated action potentials through activation of Ca-dependent K^+ channels.

To our knowledge however, there are no studies on the regulation of subcellular localization of Ca channels in the vertebrate retina. The actin-dependent internalization of $Ca_v1.3$ (but not $Ca_v1.2$) channels observed in the present study is in accord with earlier molecular studies, which indicate that

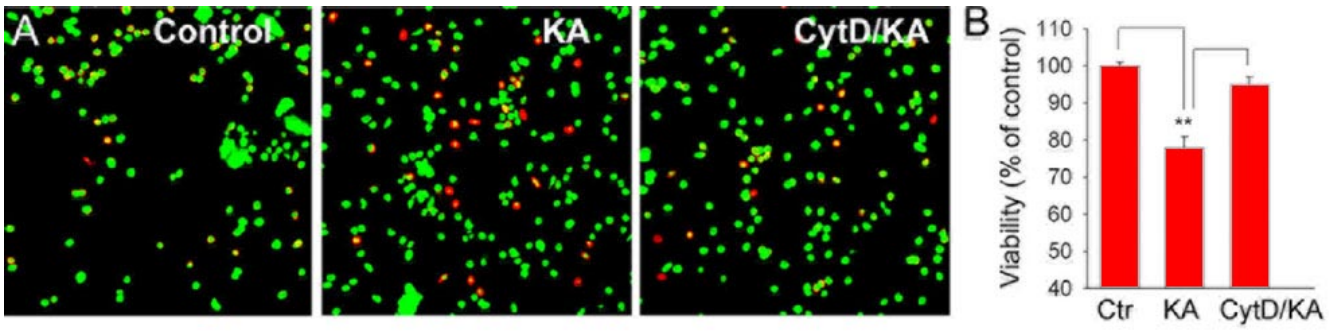

Figure 8. The effect of F-actin disruption on survival of retinal neurons in glutamate-induced excitotoxicity. Dissociated cell were incubated for 30 min in either normal Ringer solution **A**, **B** or Ringer solution containing 10 μM cytD (**C**) prior to exposure for 30 min to 100 μM kainate (**B**, **C**). Cells were then washed for 2 h and stained for live/dead assay. Calcein (green) stained healthy cells, whereas ethidium homodimer (red) stained dead cells. **D**: Cell viability was measured as the ratio of (live cells/total cells) x100, and normalized to control values (3 independent experiments).

$Ca_v1.3$ channels (but not $Ca_v1.2$) are associated with the synaptic scaffolding protein ProSAP/Shank that interacts simultaneously with different GluR complexes, the actin cytoskeleton and signaling molecules in the post synaptic densities [31].

It is becoming evident that dynamin-dependent endocytosis of plasma membrane proteins is an important means of controlling the cell surface expression, and hence function, of these proteins [26]. The distribution of three proteins important for agonist-mediated endocytosis, dynamin, amphiphysin, and clathrin has been demonstrated both in goldfish and mouse retina [32]. Dynamin-dependent internalization of AMPA receptors was recently demonstrated in mouse retina [19]. In the present study, an inhibition of endocytosis by DIP attenuated the effect of actin-depolymerizing agents on $Ca_v1.3$ channel internalization, indicating that the process was mediated through a dynamin-dependent pathway.

We have shown earlier that depolymerization of F-actin reduces L-type I_{Ca} in salamander retinal ganglion cells [23]. Here we obtained data suggesting that the inhibition of I_{Ca} is caused (at least partially) by a reduction in the number of functional Ca^{2+} channels, resulting from internalization following F-actin disruption.

What are the potential physiological role of postsynaptic Ca channels and their F-actin-regulated internalization in retinal neurons? Voltage-gated Ca channels in postsynaptic cells are implicated in the regulation of intrinsic excitability (e.g. by controlling Ca-dependent K^+ currents), which determines the probability that an EPSP will elicit an action potential. Such plasticity appears to be of fundamental importance because it directly affects the input-output function of the neuron, hence the synaptic efficacy. Furthermore, postsynaptic L-type channels, which are prominent targets for neurotransmitter-mediated regulation [33,34], are the main source for Ca^{2+} entry that triggers various Ca-dependent intracellular signaling cascades. Elevation of intracellular Ca^{2+} has been shown to regulate neurotransmitter-induced currents and light-evoked EPSCs in retinal ganglion cells [1].

Studies indicate that L-type currents resulting from expression of neuronal or cardiac $Ca_v1.2$ and $Ca_v1.3$ isoforms do not exhibit the voltage-dependent G-protein inhibition that is typical of N or P/Q type currents [35]. Instead, there is an additional mechanism for modulation of L-type channels that is not voltage-dependent and is mediated by agonist-induced Ca channel trafficking across the plasma membrane [20-22,36]. We reported recently that in salamander retinal neurons Ca^{2+} entry through either voltage-gated or a glutamate receptor-activated channel is able to induce depolymerization of F-actin [37], which in turn reduces the number of functional Ca^{2+} channels on the surface membrane (present study). Together, these data suggest that Ca^{2+} channel internalization, following F-actin depolymerization, contributes to the inhibitory action of glutamate on L-type I_{Ca}. It is not excluded however, that different regulatory pathways (voltage-dependent and voltage-independent) could be involved in the modulation of Ca^{2+} channels by a single neurotransmitter under variable physiological conditions.

We reported earlier that disruption of F-actin reduces Ca^{2+} influx through glutamate receptor-activated channels [24]. Furthermore, our experiments using a live/dead assay indicate that depolymerization of actin filaments by cytD can stabilize intracellular free Ca^{2+} levels. Together these data suggest that F-actin reorganization may play a key role protecting retinal neurons against excitotoxic injury. These data are in agreement with earlier reports on hippocampal neurons in which cytD protected neurons against glutamate-induced excitotoxic injury, whereas F-actin stabilization by jasplakinolide potentiated cell death [38]. One possible explanation for cytochalasin action on retinal cell survival is that glutamate-induced disruption of F-actin [37] opposed an elevation of internal Ca^{2+} by (i) internalizing L-type Ca channels (present study), and/or (ii) by reducing Ca^{2+} entry through glutamate receptor-activated channels [24], in this way serving as a negative feedback mechanism to protect neurons against excitotoxic cell damage.

ACKNOWLEDGEMENTS

We thank Dr. P. Witkovsky for critically reading the manuscript. This research was supported by the NIH grant EY 12497 to AA.

REFERENCES

1. Akopian A, Witkovsky P. Calcium and retinal function. Mol Neurobiol 2002; 25:113-32.
2. Catterall WA, Perez-Reyes E, Snutch TP, Striessnig J. International Union of Pharmacology. XLVIII. Nomenclature and structure-function relationships of voltage-gated calcium channels. Pharmacol Rev 2005; 57:411-25.
3. Randall A, Benham CD. Recent advances in the molecular understanding of voltage-gated Ca2+ channels. Mol Cell Neurosci 1999; 14:255-72. Erratum in: Mol Cell Neurosci 2000; 15:112.
4. Kamphuis W, Hendriksen H. Expression patterns of voltage-dependent calcium channel alpha 1 subunits (alpha 1A-alpha 1E) mRNA in rat retina. Brain Res Mol Brain Res 1998; 55:209-20.
5. Firth SI, Morgan IG, Boelen MK, Morgans CW. Localization of voltage-sensitive L-type calcium channels in the chicken retina. Clin Experiment Ophthalmol 2001; 29:183-7.
6. Xu HP, Zhao JW, Yang XL. Expression of voltage-dependent calcium channel subunits in the rat retina. Neurosci Lett 2002; 329:297-300.
7. Welch NC, Wood S, Jollimore C, Stevens K, Kelly ME, Barnes S. High-voltage-activated calcium channels in Muller cells acutely isolated from tiger salamander retina. Glia 2005; 49:259-74.
8. Henderson D, Doerr TA, Gottesman J, Miller RF. Calcium channel immunoreactivity in the salamander retina. Neuroreport 2001; 12:1493-9.
9. Logiudice L, Henry D, Matthews G. Identification of calcium channel alpha1 subunit mRNA expressed in retinal bipolar neurons. Mol Vis 2006; 12:184-9.
10. Witkovsky P, Shen C, McRory J. Differential distribution of voltage-gated calcium channels in dopaminergic neurons of the rat retina. J Comp Neurol 2006; 497:384-96.
11. Morgans CW, Gaughwin P, Maleszka R. Expression of the alpha1F calcium channel subunit by photoreceptors in the rat retina. Mol Vis 2001; 7:202-9.
12. Bech-Hansen NT, Naylor MJ, Maybaum TA, Pearce WG, Koop B, Fishman GA, Mets M, Musarella MA, Boycott KM. Loss-

of-function mutations in a calcium-channel alpha1-subunit gene in Xp11.23 cause incomplete X-linked congenital stationary night blindness. Nat Genet 1998; 19:264-7.
13. Koschak A, Reimer D, Huber I, Grabner M, Glossmann H, Engel J, Striessnig J. alpha 1D (Cav1.3) subunits can form l-type Ca2+ channels activating at negative voltages. J Biol Chem 2001; 276:22100-6.
14. Wilkinson MF, Barnes S. The dihydropyridine-sensitive calcium channel subtype in cone photoreceptors. J Gen Physiol 1996; 107:621-30.
15. Taylor WR, Morgans C. Localization and properties of voltage-gated calcium channels in cone photoreceptors of Tupaia belangeri. Vis Neurosci 1998; 15:541-52.
16. Morgans CW, Bayley PR, Oesch NW, Ren G, Akileswaran L, Taylor WR. Photoreceptor calcium channels: insight from night blindness. Vis Neurosci 2005; 22:561-8.
17. Malinow R, Malenka RC. AMPA receptor trafficking and synaptic plasticity. Annu Rev Neurosci 2002; 25:103-26.
18. Lai HC, Jan LY. The distribution and targeting of neuronal voltage-gated ion channels. Nat Rev Neurosci 2006; 7:548-62.
19. Xia Y, Carroll RC, Nawy S. State-dependent AMPA receptor trafficking in the mammalian retina. J Neurosci 2006; 26:5028-36.
20. Altier C, Khosravani H, Evans RM, Hameed S, Peloquin JB, Vartian BA, Chen L, Beedle AM, Ferguson SS, Mezghrani A, Dubel SJ, Bourinet E, McRory JE, Zamponi GW. ORL1 receptor-mediated internalization of N-type calcium channels. Nat Neurosci 2006; 9:31-40.
21. Puckerin A, Liu L, Permaul N, Carman P, Lee J, Diverse-Pierluissi MA. Arrestin is required for agonist-induced trafficking of voltage-dependent calcium channels. J Biol Chem 2006; 281:31131-41.
22. Tombler E, Cabanilla NJ, Carman P, Permaul N, Hall JJ, Richman RW, Lee J, Rodriguez J, Felsenfeld DP, Hennigan RF, Diverse-Pierluissi MA. G protein-induced trafficking of voltage-dependent calcium channels. J Biol Chem 2006; 281:1827-39.
23. Schubert T, Akopian A. Actin filaments regulate voltage-gated ion channels in salamander retinal ganglion cells. Neuroscience 2004; 125:583-90.
24. Akopian A, Szikra T, Cristofanilli M, Krizaj D. Glutamate-induced Ca2+ influx in third-order neurons of salamander retina is regulated by the actin cytoskeleton. Neuroscience 2006; 138:17-24.
25. Hell JW, Westenbroek RE, Warner C, Ahlijanian MK, Prystay W, Gilbert MM, Snutch TP, Catterall WA. Identification and differential subcellular localization of the neuronal class C and class D L-type calcium channel alpha 1 subunits. J Cell Biol 1993; 123:949-62.
26. Le Roy C, Wrana JL. Clathrin- and non-clathrin-mediated endocytic regulation of cell signalling. Nat Rev Mol Cell Biol 2005; 6:112-26.
27. Wigge P, McMahon HT. The amphiphysin family of proteins and their role in endocytosis at the synapse. Trends Neurosci 1998; 21:339-44.
28. Luscher C, Xia H, Beattie EC, Carroll RC, von Zastrow M, Malenka RC, Nicoll RA. Role of AMPA receptor cycling in synaptic transmission and plasticity. Neuron 1999; 24:649-58.
29. Sucher NJ, Lipton SA, Dreyer EB. Molecular basis of glutamate toxicity in retinal ganglion cells. Vision Res 1997; 37:3483-93.
30. Morgans CW. Calcium channel heterogeneity among cone photoreceptors in the tree shrew retina. Eur J Neurosci 1999; 11:2989-93.
31. Boeckers TM. The postsynaptic density. Cell Tissue Res 2006; 326:409-22.
32. Sherry DM, Heidelberger R. Distribution of proteins associated with synaptic vesicle endocytosis in the mouse and goldfish retina. J Comp Neurol 2005; 484:440-57.
33. Akopian A, Witkovsky P. Activation of metabotropic glutamate receptors decreases a high-threshold calcium current in spiking neurons of the Xenopus retina. Vis Neurosci 1996; 13:549-57.
34. Shen W, Slaughter MM. Metabotropic and ionotropic glutamate receptors regulate calcium channel currents in salamander retinal ganglion cells. J Physiol 1998; 510:815-28.
35. Bell DC, Butcher AJ, Berrow NS, Page KM, Brust PF, Nesterova A, Stauderman KA, Seabrook GR, Nurnberg B, Dolphin AC. Biophysical properties, pharmacology, and modulation of human, neuronal L-type (alpha(1D), Ca(V)1.3) voltage-dependent calcium currents. J Neurophysiol 2001; 85:816-27.
36. Diverse-Pierluissi M, Dunlap K. Distinct, convergent second messenger pathways modulate neuronal calcium currents. Neuron 1993; 10:753-60.
37. Cristofanilli M, Akopian A. Calcium channel and glutamate receptor activities regulate actin organization in salamander retinal neurons. J Physiol 2006; 575:543-54.
38. Furukawa K, Smith-Swintosky VL, Mattson MP. Evidence that actin depolymerization protects hippocampal neurons against excitotoxicity by stabilizing [Ca2+]i. Exp Neurol 1995; 133:153-63.

The print version of this article was created on 28 Aug 2007. This reflects all typographical corrections and errata to the article through that date. Details of any changes may be found in the online version of the article.